



# Modeling dislocation absorption by surfaces within the framework of strain gradient crystal plasticity



Xiang-Long Peng, Gan-Yun Huang\*

Tianjin Key Laboratory of Modern Engineering Mechanics, Department of Mechanics, School of Mechanical Engineering, Tianjin University, Tianjin 300072, PR China

## ARTICLE INFO

### Article history:

Received 22 January 2015

Received in revised form 13 July 2015

Available online 22 July 2015

### Keywords:

Size effect

Dislocation absorption

Surface steps

Strain gradient

Crystal plasticity

## ABSTRACT

Surfaces play important roles in plastic deformation of crystals at submicron scale by emitting/absorbing dislocations and hence may contribute to the complicated size effect. To take into account the dislocation absorption on the continuum level, an energetic surface model has been proposed by considering the change of surface energy contributed by the formation of surface steps via dislocation absorption. In combination with the conventional higher-order strain gradient theory for grain interior, a new model for single crystal plasticity has been developed. Within the model, there exists a critical threshold for the onset of dislocation absorption by surfaces, alternatively, an independent yield criterion for surfaces and the microscopic boundary conditions can be obtained naturally. As an example of application, plastic behavior of a thin film under plane constrained shear has been studied. Results demonstrate that surface yield strength strongly depends on the film thickness and the orientation of the activated slip system. Comparison with the strain gradient plasticity models under the conventional microscopic boundary conditions, i.e., the microhard and microfree conditions has also been made. It has been found that the plastic behavior is sensitive to the surface boundary conditions.

© 2015 Elsevier Ltd. All rights reserved.

## 1. Introduction

The rapid development of small-scale devices such as those in micro-electromechanical systems (MEMs) and high performance structures has triggered intensive research on the mechanical properties of materials at micron and submicron scales to ensure the stability and reliability during practical applications. As observed in many experiments such as the micro-torsion of thin metallic wires (e.g., Fleck et al. (1994)), the micro- and nanoindentation experiments (e.g., McElhane et al. (1998) and Swadener et al. (2002)) and the compression of micropillars (e.g., Gu et al. (2012)), different from their bulk counterparts, plastic behaviors of crystalline materials at small scales are usually size-dependent. Due to the lack of the material length scales, conventional plasticity theories are incapable of predicting such size effects. Thus, the scale-dependent plasticity theories are desired. To this end, various strain gradient plasticity theories have been developed by considering the effect of plastic strain gradient since the pioneering work by Aifantis (1984). According to Kuroda and Tvergaard (2008), there are two approaches to incorporate the plastic strain gradient into the constitutive law. One is to assume

a plastic strain gradient enhanced work-hardening law within the framework of conventional plasticity theories, resulting in the lower-order strain gradient plasticity theories (e.g., Acharya and Bassani (2000), Chen and Wang (2000), Evers et al. (2002), and Han et al. (2005)) with the same governing equations as those in conventional theories, thus no additional boundaries other than surface traction or prescribed displacement conditions are needed. The other approach or alternatively the higher-order strain gradient theory is achieved by introducing higher-order stress which is the work-conjugate of plastic strain gradient (e.g., Fleck and Hutchinson (1993, 1997) and Gurtin (2000, 2002)) or higher-order equations associated with dislocation density (e.g., Groma et al. (2003), Yefimov et al. (2004), Evers et al. (2004), and Bayley et al. (2006)).

In the higher-order strain gradient theories, additional microscopic boundary conditions for the higher-order governing equations are needed. To date, the microhard and the microfree conditions are usually adopted. The former corresponds to the situations when the surface/interface acts as barriers to dislocation motion and hence makes the plastic strain vanishing therein. It is also termed as the condition of impenetrable surface/interface in the literature. Conversely, the microfree condition implies that the surface/interface allows free penetration of dislocations so that the density of geometrical necessary dislocations (GNDs) or the

\* Corresponding author. Tel.: +86 22 27404934.

E-mail address: [gyhuang@tju.edu.cn](mailto:gyhuang@tju.edu.cn) (G.-Y. Huang).

higher-order tractions are prescribed to be zero. However, the practical situations may be beyond the capture of such boundary conditions although they represent the two extreme cases. Actually, taking advantage of atomistic simulations, Van Swygenhoven et al. (2002), Spearot et al. (2005), and Yuasa et al. (2010) have found in nanocrystalline materials that grain boundaries emit and absorb dislocations instead of acting as barriers to the motion of dislocations. Compelling evidence for dislocations escape towards and nucleation at the surface has been observed in experiments (Shan et al., 2008; Oh et al., 2009) and atomistic simulations (e.g., Rabkin and Srolovitz (2007)) on submicron sized crystals. More works on the interaction mechanisms between dislocations and surface/interface through atomistic simulations and experiments may be found in the reviews recently made by Spearot and Sangid (2014) and Kacher et al. (2014). Moreover, deformation mechanisms such as grain boundary sliding, migration and twinning initiated at the grain boundaries have been discovered to be important or even dominant in nanocrystalline materials (Wang et al., 2012a; Rajabzadeh et al., 2013). To capture those deformation processes and for the strain gradient plasticity to be applicable, a decent formulation of boundary conditions for the surface/interface in small-scaled crystalline materials is necessary.

Within the framework of strain gradient crystal plasticity, Cermelli and Gurtin (2002) have firstly addressed the role of surface/interface. They developed a slip rate and higher-order stresses dependent interface model by considering the dissipative nature of grain boundary processes. The model indeed results in discontinuous higher-order tractions and slip rates over the interface. It was subsequently modified by Gurtin and Needleman (2005) so as to render the higher-order tractions continuous over the interface. Recognizing that dislocations accumulating at surface/interface influence its energetic state, which can be modeled by a surface energy that depends on the plastic strain state at both sides of the interface, Gudmundson and co-workers (Gudmundson, 2004; Fredriksson and Gudmundson, 2005, 2007) developed an energetic model that gives consistent boundary conditions for the problems defined by strain gradient theories. By assuming interfaces behave similarly as the grain interior, Aifantis et al. (2006) have proposed an interface potential that depends on the plastic strain at the interface up to the quadratic terms. It results in a yield-like condition at an interface. Similar energetic interface model has been adopted by Abu AL-Rub (2008) to consider the yield strength and flow stress of thin film substrate system. From those works it can be found that consistent boundary conditions can be defined by introducing plastic deformation dependent of interface energy. Nevertheless, without account of the underlying physical mechanisms, the additional parameters thus introduced can hardly be estimated. Based on the formation of steps due to dislocation absorption by surfaces, Huang and Svendsen (2010) have proposed a plastic deformation dependent surface model for thin films. Hurtado and Ortiz (2012) have obtained an explicit relation between the plastic strain at the surface and the area of surface steps due to dislocation absorption, and hence a surface model that depends on the plastic strain linearly has been derived with the surface parameter explicitly denoted by the specific surface-step energy. The surface models as shown by the results capture well some size dependent features in the plastic deformation of crystalline materials at submicron scale.

Dislocation absorption by surfaces may induce mechanical annealing and may be closely related to the dislocation starvation as revealed in some recent experiments (Shan et al., 2008; Wang et al., 2012b). Given the success of strain gradient theories with impenetrable boundaries in explaining the size effect of microstructured crystals, one may naturally ask when dislocation

absorption occurs and how it may contribute to the strain hardening. To address such questions, strain gradient plasticity with proper surface model is necessary. The surface models as aforementioned may be inadequate since they depend on the plastic deformation linearly which implies step density due to dislocation absorption may be small. Indeed, as illustrated in many works (e.g., Marchenko and Parshin (1980) and Prévot and Croset (2004, 2006)), the surface steps may interact with each other elastically, which contributes to surface energy. Further, Sieradzki et al. (2006) have pointed out that the elastic interaction between surface steps may serve as a source of hardening in plastic deformation. Therefore, the interaction energy between surface steps should also be taken into account. Taken those together, the present authors would like to formulate a physically based energetic surface model in combination with a strain gradient model for the grain interior so as to capture the surface relevant deformation process and the size effect in crystal deformation. To that end, the paper is organized as follows. To start with, in Section 2 a physically based single crystal strain gradient theory is summarized based on the models of Gurtin (2002), Evers et al. (2004) and Bayley et al. (2006), and the surface energy density based on the formation and interaction of surface steps is derived. In Section 3, the formulated model is applied to study the plastic behavior of single crystalline thin films under plane constrained shear. The conclusions are made in Section 4.

## 2. A strain gradient model with account of dislocation absorption by surfaces

### 2.1. Kinematics basis of single crystal plasticity

In crystal plasticity, the fundamental kinematic field quantities include the displacements and the slip on individual slip systems. In the current work, we consider a single crystal containing a set of slip systems each of which is defined by a slip plane normal  $\mathbf{m}^\alpha$  and a slip direction  $\mathbf{s}^\alpha$ . The total distortion can be decomposed into elastic and plastic parts as

$$\mathbf{H} = \mathbf{u}\nabla = \mathbf{H}^e + \mathbf{H}^p \quad (1)$$

where the plastic distortion  $\mathbf{H}^p$  is defined as the sum over all active slip systems, i.e.,

$$\mathbf{H}^p = \sum_{\alpha} \gamma^{\alpha} \mathbf{s}^{\alpha} \otimes \mathbf{m}^{\alpha} \quad (2)$$

with  $\gamma^{\alpha}$  being the slip on slip system  $\alpha$ . Thus, the total strain  $\boldsymbol{\varepsilon}$  is defined as the symmetric part of the total distortion, i.e.,

$$\boldsymbol{\varepsilon} = \frac{1}{2}(\mathbf{H}^e + \mathbf{H}^{eT}) + \frac{1}{2}(\mathbf{H}^p + \mathbf{H}^{pT}) = \boldsymbol{\varepsilon}^e + \boldsymbol{\varepsilon}^p \quad (3)$$

in which  $\boldsymbol{\varepsilon}^e$  and  $\boldsymbol{\varepsilon}^p$  is the elastic and plastic strain respectively.

GNDs density is a central quantity to the strain gradient crystal plasticity theory. As described in many works (e.g., Gurtin (2002)), the GNDs densities of edge and screw characters for slip system  $\alpha$ , denoted by  $\rho_G^{\alpha(e)}$  and  $\rho_G^{\alpha(s)}$ , respectively, can be expressed as

$$\rho_G^{\alpha(e)} = -\frac{1}{b} \nabla \gamma^{\alpha} \cdot \mathbf{s}^{\alpha}, \quad \rho_G^{\alpha(s)} = \frac{1}{b} \nabla \gamma^{\alpha} \cdot \mathbf{p}^{\alpha} \quad (4)$$

where  $\mathbf{p}^{\alpha} = \mathbf{s}^{\alpha} \times \mathbf{m}^{\alpha}$  and  $b$  is the magnitude of the Burgers vector.

### 2.2. Mechanical balance equations

Within the framework of strain gradient theories, according to Gurtin (2002), the internal power which is expended independently on the elastic strain rate, the slip rate and its gradient can be written as

$$P^{\text{int}} = \int_V \boldsymbol{\sigma} : \dot{\boldsymbol{\varepsilon}}^e dV + \sum_{\alpha} \int_V (\pi^{\alpha} \dot{\gamma}^{\alpha} + \xi^{\alpha} \cdot \nabla \dot{\gamma}^{\alpha}) dV + \sum_{\alpha} \int_S \eta^{\alpha} \dot{\gamma}^{\alpha} dS \quad (5)$$

where  $\boldsymbol{\sigma}$  is the Cauchy stress,  $\pi^{\alpha}$  and  $\xi^{\alpha}$  are respectively the microforces and the microstresses that are work-conjugates of the slip  $\gamma^{\alpha}$  and the slip gradient  $\nabla \gamma^{\alpha}$ , and  $\eta^{\alpha}$  are microforces being work-conjugates of slip  $\gamma^{\alpha}$  at the surface of the body. Note that the last term in Eq. (5) contributed by the power of microforces at the surface is ignored in Gurtin (2002). The external power in the absence of body force is given as

$$P^{\text{ext}} = \int_S \mathbf{T} \cdot \dot{\mathbf{u}} dS + \sum_{\alpha} \int_S \Xi^{\alpha} \dot{\gamma}^{\alpha} dS \quad (6)$$

with  $\mathbf{T}$  and  $\Xi^{\alpha}$  being the externally applied standard traction and the microtraction (or higher-order traction), respectively. Equating the variation of internal power  $P^{\text{int}}$  to the external power  $P^{\text{ext}}$  yields the following virtual power relation

$$\begin{aligned} \int_V \boldsymbol{\sigma} : \delta \dot{\boldsymbol{\varepsilon}}^e dV + \sum_{\alpha} \int_V (\pi^{\alpha} \delta \dot{\gamma}^{\alpha} + \xi^{\alpha} \cdot \nabla \delta \dot{\gamma}^{\alpha}) dV + \sum_{\alpha} \int_S \eta^{\alpha} \delta \dot{\gamma}^{\alpha} dS \\ = \int_S \mathbf{T} \cdot \delta \dot{\mathbf{u}} dS + \sum_{\alpha} \int_S \Xi^{\alpha} \delta \dot{\gamma}^{\alpha} dS \end{aligned} \quad (7)$$

Given the validity of Eq. (7) for arbitrary  $\delta \dot{\gamma}^{\alpha}$ , the macroscopic balance equation can be obtained as

$$\nabla \cdot \boldsymbol{\sigma} = \mathbf{0} \quad (8)$$

and the corresponding standard traction condition

$$\boldsymbol{\sigma} \cdot \mathbf{N} = \mathbf{T} \quad (9)$$

with  $\mathbf{N}$  being the surface outward normal. Then, considering null virtual displacement yields the microscopic balance equations

$$\mathbf{s}^{\alpha} \cdot \boldsymbol{\sigma} \cdot \mathbf{m}^{\alpha} + \nabla \cdot \xi^{\alpha} - \pi^{\alpha} = 0 \quad (10)$$

and the associated microscopic boundary conditions

$$\xi^{\alpha} \cdot \mathbf{N} + \eta^{\alpha} = \Xi^{\alpha} \quad (11)$$

Generally, the power of the microforces  $\eta^{\alpha}$  at the surface, i.e., the last term in Eq. (5), may consist of the energetic part and the dissipative part, and the latter is neglected here. Thus, according to the dissipation inequality and the assumption that there is no dissipative energy at the surface,  $\int_S (\sum_{\alpha} \eta^{\alpha} \dot{\gamma}^{\alpha} - \dot{\psi}^s) dS = 0$  should be satisfied if the density of surface energy  $\psi^s$  is introduced, which leads to  $\eta^{\alpha} = \partial \psi^s / \partial \gamma^{\alpha}$ .

### 2.3. Bulk constitutive laws

The Cauchy stress  $\boldsymbol{\sigma}$  defined here is consistent with the conventional linear elasticity theory and the associated constitutive relation is

$$\boldsymbol{\sigma} = \mathbf{C} : \boldsymbol{\varepsilon}^e \quad (12)$$

where  $\mathbf{C}$  is the fourth order elastic tensor. For isotropic materials considered in the present work, the constitutive law can be rewritten as

$$\boldsymbol{\sigma} = 2\mu \boldsymbol{\varepsilon}^e + \lambda \text{tr}(\boldsymbol{\varepsilon}^e) \mathbf{I} \quad (13)$$

where  $\lambda$  and  $\mu$  are the Lamé constants.

As illustrated by Kuroda and Tvergaard (2008) and Ertürk et al. (2009), the microstress  $\xi^{\alpha}$  in Eq. (10) is related to the back stress  $\tau_b^{\alpha}$  in Evers et al. (2004) and Bayley et al. (2006) via

$$\tau_b^{\alpha} = -\nabla \cdot \xi^{\alpha} \quad (14)$$

According to Evers et al. (2004) and Bayley et al. (2006), the back stress  $\tau_b^{\alpha}$  accounts for the long range interaction between GNDs, and can be expressed as

$$\tau_b^{\alpha} = -\mathbf{s}^{\alpha} \cdot \boldsymbol{\sigma}^{\text{int}} \cdot \mathbf{m}^{\alpha} \quad (15)$$

where  $\boldsymbol{\sigma}^{\text{int}}$  is the internal stress induced by the long range interaction between GNDs.  $\boldsymbol{\sigma}^{\text{int}}$  can be derived based on the stress field of a single edge or screw dislocation in an infinite elastic solid, and for details one is referred to Evers et al. (2004) and Bayley et al. (2006). It is worthwhile to mention that Evers et al. (2004) considered only the interaction between GNDs within the same slip system and the interaction between those from different slip systems has been ignored. By taking into account the interaction between different slip systems as well,  $\boldsymbol{\sigma}^{\text{int}}$  according to Bayley et al. (2006) can be expressed as

$$\boldsymbol{\sigma}^{\text{int}} = \frac{\mu b R^2}{8(1-\nu)} \sum_{\beta} \nabla \rho_G^{\beta(e)} \cdot \mathbf{M}^{\beta(e)} + \frac{\mu b R^2}{4} \sum_{\beta} \nabla \rho_G^{\beta(s)} \cdot \mathbf{M}^{\beta(s)} \quad (16)$$

where  $\nu$  is Poisson's ratio  $R$ , is a bulk characteristic length scale denoting the radius of a domain within which the GNDs interaction is considered, and  $\mathbf{M}^{\beta(e)}$  and  $\mathbf{M}^{\beta(s)}$  are the third order tensors related to the orientation of slip system for edge and screw characters, respectively, i.e.,

$$\begin{aligned} \mathbf{M}^{\beta(e)} &= 3\mathbf{m}^{\beta} \mathbf{s}^{\beta} \mathbf{s}^{\beta} + \mathbf{m}^{\beta} \mathbf{m}^{\beta} \mathbf{m}^{\beta} + 4\nu \mathbf{m}^{\beta} \mathbf{p}^{\beta} \mathbf{p}^{\beta} - \mathbf{s}^{\beta} \mathbf{s}^{\beta} \mathbf{m}^{\beta} - \mathbf{s}^{\beta} \mathbf{m}^{\beta} \mathbf{s}^{\beta}, \\ \mathbf{M}^{\beta(s)} &= -\mathbf{m}^{\beta} \mathbf{p}^{\beta} \mathbf{s}^{\beta} - \mathbf{m}^{\beta} \mathbf{s}^{\beta} \mathbf{p}^{\beta} + \mathbf{p}^{\beta} \mathbf{s}^{\beta} \mathbf{m}^{\beta} + \mathbf{p}^{\beta} \mathbf{m}^{\beta} \mathbf{s}^{\beta} \end{aligned} \quad (17)$$

Substituting Eqs. (15) and (16) into Eq. (14) yields the constitutive law for microstress  $\xi^{\alpha}$  (Ertürk et al., 2009)

$$\xi^{\alpha} = \left( \frac{\mu b R^2}{8(1-\nu)} \sum_{\beta} \rho_G^{\beta(e)} \mathbf{M}^{\beta(e)} + \frac{\mu b R^2}{4} \sum_{\beta} \rho_G^{\beta(s)} \mathbf{M}^{\beta(s)} \right) : \mathbf{s}^{\alpha} \mathbf{m}^{\alpha} \quad (18)$$

The microforce  $\pi^{\alpha}$  according to Evers et al. (2004) and Bayley et al. (2006) is interpreted as a slip resistance due to the short range dislocations interactions. In the current work, for simplicity, we ignore the slip resistance, thus

$$\pi^{\alpha} = 0. \quad (19)$$

### 2.4. Formulation of a new surface model and boundary conditions

#### 2.4.1. Surface boundary conditions

To complete the formulation of the boundary value problems defined by strain gradient plasticity, proper boundary conditions are necessary. Macroscopically, displacement  $\mathbf{u}^0$  may be imposed on the surface  $S^u$  and/or traction  $\mathbf{T}^0$  may be exerted on the surface  $S^T$ , which may give

$$\begin{aligned} \mathbf{u} &= \mathbf{u}^0, \quad \text{at } S^u \\ \boldsymbol{\sigma} \cdot \mathbf{N} &= \mathbf{T}^0, \quad \text{at } S^T \end{aligned} \quad (20)$$

for the macroscopic surface boundary conditions. For the boundary conditions specific to the high-order crystal plasticity strain gradient theories, either microhard condition or microfree condition is usually adopted. The former means that the surface/interface acts as barrier to dislocation motion, which leads to

$$\gamma^{\alpha} = 0 \quad (21)$$

The latter corresponds to the situation when a surface is free for dislocations to penetrate, thus higher-order stresses are prescribed to be zero at the boundaries. i.e.,

$$\xi^{\alpha} \cdot \mathbf{N} = 0 \quad (22)$$

The conditions specified by Eqs. (21) and (22) may represent two extreme cases. In practice, surfaces and interfaces may emit or absorb dislocations, which in turn results in the formation of surface defects such as surface steps and is beyond capture by the two equations. As a result of the formation of steps on an

otherwise flat surface, surface energy will change with plastic deformation, and the corresponding proper microscopic boundary conditions may be expressed by Eq. (11). In the present work, we consider that only the conventional traction can be applied and hence  $\Xi^\alpha = 0$ , then the microscopic boundary conditions Eq. (11) can be rewritten as

$$\xi^\alpha \cdot \mathbf{N} = -\frac{\partial \psi^s}{\partial \gamma^\alpha} \quad (23)$$

In the following, we will derive a physically motivated expression for the density of surface energy  $\psi^s$  by considering the interaction between dislocation and surfaces due to the formation of steps.

#### 2.4.2. Surface energy due to dislocations absorption by surfaces

According to Eq. (23), the microtractions at surfaces or boundaries are governed by plastic deformation dependent surface energy density. To study when the initiation of mechanical annealing (Shan et al., 2008; Wang et al., 2012b) occurs and its effect, an explicit expression for the surface energy density is required. Either emission or absorption of dislocations at the surface generates the surface steps. On the one hand, the formation of steps increases the surface area and hence the surface free energy. On the other hand, the multiple surface steps interact with each other leading to additional interaction energy that also contributes to the surface energy as described in many works (e.g., Marchenko and Parshin (1980) and Prévot and Croset (2004, 2006)). Therefore, the surface energy density  $\psi^s$  due to surface steps can be expressed as

$$\psi^s = \psi_{sur}^s + \psi_{el}^s \quad (24)$$

where  $\psi_{sur}^s$  represents the density of surface free energy arising from the change of surface area and  $\psi_{el}^s$  accounts for the interaction energy induced by steps per unit surface area. In fact, Hurtado and Ortiz (2012) have already proposed an energetic surface model based on steps induced increase of surface area but the interaction energy has been neglected. According to their work,  $\psi_{sur}^s$  is proportional to the slip. As pointed out by Sieradzki et al. (2006), the elastic interaction between surface steps may serve as a source of hardening. Thus  $\psi_{el}^s$  should also be taken into account. In the following, the expressions for  $\psi_{sur}^s$  and  $\psi_{el}^s$  will be derived respectively.

Based on the work of Hurtado and Ortiz (2012), let us consider a slip system  $\alpha$  abutting on an element of a surface with outward normal  $\mathbf{N}$ . Denoting the distance between two adjacent activated parallel slip planes and the slip displacement on each slip planes in the direction of Burgers vector as  $L^\alpha$  and  $\delta^\alpha$  respectively, then the slip  $\gamma^\alpha$ , the width of one step and the step spacing can be respectively expressed as

$$\gamma^\alpha = \frac{\delta^\alpha}{L^\alpha}, \quad (25)$$

$$w^\alpha = |\delta^\alpha| \frac{|\mathbf{s}^\alpha \cdot \mathbf{N}|}{|\mathbf{m}^\alpha \times \mathbf{N}|}, \quad (26)$$

$$d^\alpha = \frac{L^\alpha}{|\mathbf{m}^\alpha \times \mathbf{N}|}. \quad (27)$$

By taking advantage of the above identities, the surface step area per unit surface area contributed by slip system  $\alpha$  reads

$$S^\alpha = \frac{w^\alpha}{d^\alpha} = |\gamma^\alpha| |\mathbf{s}^\alpha \cdot \mathbf{N}|. \quad (28)$$

So the total surface step area per unit surface area from all the slip systems can be obtained as

$$S = \sum_\alpha S^\alpha = \sum_\alpha |\gamma^\alpha| |\mathbf{s}^\alpha \cdot \mathbf{N}| \quad (29)$$

If denoting  $\Gamma_1^\alpha$  as the free energy per unit surface step area for the slip system  $\alpha$ , one may arrive at

$$\psi_{sur}^s = \sum_\alpha \Gamma_1^\alpha |\gamma^\alpha| |\mathbf{s}^\alpha \cdot \mathbf{N}| \quad (30)$$

According to the model of Marchenko and Parshin (1980), a surface step can be adequately simulated as a force dipole. So the step-step interaction energy can be obtained by that between force dipoles. For two force dipole lines separated by a distance  $d$  and lying on the surface of a semi-infinite body, the interaction energy per unit length  $W_{int}$  can be expressed as

$$W_{int} = \frac{(1-\nu)}{\mu\pi} \frac{A_1 A_2}{d^2} \quad (31)$$

where  $A_i$  is the strength of the force dipole. For a surface step as a force dipole,  $A_i$  may be related to the step height  $h_i$  by

$$A_i = f h_i \quad (32)$$

with  $f$  being a surface stress-like material parameter. Due to the model of surface dipoles for steps, a single surface dipole will induce elastic deformation in the half plane, which implies the existence of self-energy. As discussed by Müller and Saül (2004), the self-energy  $W_{self}$  for a single step calculated by the model of Marchenko and Parshin (1980) diverges, and the conventional removal of this divergence is to introduce a cut-off distance  $a$  of the order of interatomic distance. Thus  $W_{self}$  can be approximately expressed as

$$W_{self} = \frac{1-\nu}{\mu\pi} \frac{A_i^2}{8a^2} \quad (33)$$

Based on the above argument, the steps' self-energy and the step-step interaction energy per unit surface area associated with slip system  $\alpha$  can be respectively expressed as

$$\phi_{self}^\alpha = \frac{1-\nu}{8\mu\pi a^2} \frac{(f^\alpha h^\alpha)^2}{d^\alpha} \quad (34)$$

and

$$\phi_{int}^\alpha = \frac{1-\nu}{\mu\pi} \frac{(f^\alpha h^\alpha)^2}{(d^\alpha)^3} \quad (35)$$

Since  $f^\alpha$  is the surface stress-like material parameter, it is estimated to be on the order of the magnitude of  $\Gamma_1^\alpha$ . The distance between two adjacent steps  $d^\alpha$  is assumed to be a constant during deformation, and step height  $h^\alpha$  reads

$$h^\alpha = \delta^\alpha |\mathbf{s}^\alpha \cdot \mathbf{N}| \quad (36)$$

As the interaction energy between two steps decays quickly with the step distance, we consider only the interaction between two adjacent steps. Upon substitution of Eqs. (25), (27) and (36) into Eqs. (34) and (35), one may express  $\phi_{self}^\alpha$  and  $\phi_{int}^\alpha$  as

$$\phi_{self}^\alpha = \frac{(1-\nu)(f^\alpha)^2 d^\alpha}{8\mu\pi a^2} (|\mathbf{s}^\alpha \cdot \mathbf{N}| |\mathbf{m}^\alpha \times \mathbf{N}|)^2 (\gamma^\alpha)^2 \quad (37)$$

and

$$\phi_{int}^\alpha = \frac{(1-\nu)(f^\alpha)^2}{\mu\pi d^\alpha} (|\mathbf{s}^\alpha \cdot \mathbf{N}| |\mathbf{m}^\alpha \times \mathbf{N}|)^2 (\gamma^\alpha)^2 \quad (38)$$

Combining Eq. (37) with Eq. (38) gives the total step induced elastic energy per unit surface area

$$\phi^\alpha = \phi_{self}^\alpha + \phi_{int}^\alpha = \Gamma_2^\alpha (|\mathbf{s}^\alpha \cdot \mathbf{N}| |\mathbf{m}^\alpha \times \mathbf{N}|)^2 (\gamma^\alpha)^2 \quad (39)$$

where  $\Gamma_2^\alpha = (1-\nu)(f^\alpha)^2 [(d^\alpha/a)^2 + 8]/8\mu\pi d^\alpha$  is a parameter dependent on slip systems. In fact, the steps from different slip systems



can also interact with each other, and the associated energy  $\phi^{\alpha\beta}$ , similar to the derivation for step-step interaction energy within a specified slip system, can be obtained

$$\phi^{\alpha\beta} = \Gamma^{\alpha\beta} |\mathbf{s}^\alpha \cdot \mathbf{N}||\mathbf{m}^\alpha \times \mathbf{N}||\mathbf{s}^\beta \cdot \mathbf{N}||\mathbf{m}^\beta \times \mathbf{N}|\gamma^\alpha\gamma^\beta \quad (40)$$

at which  $\Gamma^{\alpha\beta}$  assumes the form as follows

$$\Gamma^{\alpha\beta} = \frac{(1-\nu)f^\alpha f^\beta d^\alpha d^\beta}{\mu\pi (d^{\alpha\beta})^3} \quad (41)$$

with  $d^{\alpha\beta}$  being the distance between two adjacent steps from different slip systems. Noteworthy that intersecting steps are not considered. Through taking contributions from all the slip systems into account, the steps induced elastic energy per unit surface area  $\psi_{el}^s$  is expressed as

$$\begin{aligned} \psi_{el}^s &= \sum_{\alpha} \phi^{\alpha} + \frac{1}{2} \sum_{\substack{\alpha, \beta \\ \alpha \neq \beta}} \phi^{\alpha\beta} = \sum_{\alpha} \Gamma_2^{\alpha} (|\mathbf{s}^\alpha \cdot \mathbf{N}||\mathbf{m}^\alpha \times \mathbf{N}|)^2 (\gamma^\alpha)^2 \\ &\quad + \frac{1}{2} \sum_{\substack{\alpha, \beta \\ \alpha \neq \beta}} \Gamma^{\alpha\beta} |\mathbf{s}^\alpha \cdot \mathbf{N}||\mathbf{m}^\alpha \times \mathbf{N}||\mathbf{s}^\beta \cdot \mathbf{N}||\mathbf{m}^\beta \times \mathbf{N}|\gamma^\alpha\gamma^\beta \\ &= \sum_{\alpha, \beta} \lambda^{\alpha\beta} |\mathbf{s}^\alpha \cdot \mathbf{N}||\mathbf{m}^\alpha \times \mathbf{N}||\mathbf{s}^\beta \cdot \mathbf{N}||\mathbf{m}^\beta \times \mathbf{N}|\gamma^\alpha\gamma^\beta \end{aligned} \quad (42)$$

where

$$\lambda^{\alpha\beta} = \begin{cases} \Gamma_2^{\alpha} & \alpha = \beta \\ \frac{1}{2} \Gamma^{\alpha\beta} & \alpha \neq \beta \end{cases} \quad (43)$$

Substituting Eqs. (30) and (42) into Eq. (24), one may obtain the expression for the total surface energy density due to dislocation absorption as

$$\psi^s = \sum_{\alpha} \Gamma_1^{\alpha} |\gamma^\alpha| |\mathbf{s}^\alpha \cdot \mathbf{N}| + \sum_{\alpha, \beta} \lambda^{\alpha\beta} |\mathbf{s}^\alpha \cdot \mathbf{N}||\mathbf{m}^\alpha \times \mathbf{N}||\mathbf{s}^\beta \cdot \mathbf{N}||\mathbf{m}^\beta \times \mathbf{N}|\gamma^\alpha\gamma^\beta \quad (44)$$

The microscopic surface boundary condition Eq. (23) then can be explicitly expressed as

$$\xi^\alpha \cdot \mathbf{N} = - \left[ \Gamma_1^{\alpha} |\mathbf{s}^\alpha \cdot \mathbf{N}| \text{sign}(\gamma^\alpha) + \sum_{\alpha, \beta} 2\lambda^{\alpha\beta} |\mathbf{s}^\alpha \cdot \mathbf{N}||\mathbf{m}^\alpha \times \mathbf{N}||\mathbf{s}^\beta \cdot \mathbf{N}||\mathbf{m}^\beta \times \mathbf{N}|\gamma^\alpha\gamma^\beta \right] \quad (45)$$

where the terms at the right hand side and the left hand side can be interpreted as the driving force and the resistance for dislocations to penetrate the surface. Thus when the driving force is not large enough, dislocations cannot be absorbed by the surface. In such a sense, the present model naturally consists of a critical loading for the onset of dislocation absorption by surfaces, namely a yield condition for the surface. It is similar to the phenomenological model for interfaces by Aifantis et al. (2006) that produced results in good agreement with some indentation experiments. But herein values for  $\Gamma_1^{\alpha}$  and  $\lambda^{\alpha\beta}$  can be reasonably estimated. The critical loading for the onset of dislocation absorption by surfaces can be determined from

$$|\xi^\alpha \cdot \mathbf{N}| = \Gamma_1^{\alpha} |\mathbf{s}^\alpha \cdot \mathbf{N}| \quad (46)$$

The underlying assumption is that before the surface yielding, plastic deformation at the surface should be zero and the microhard conditions Eq. (21) should be adopted. Once the surface yielding happens, the surface boundary conditions should be replaced by Eq. (45) and at the critical loading vanishing surface plastic deformation leads to Eq. (46).

From the derivation of the present surface model, it can be seen that the physical meaning of surface relevant material parameters is evident and hence they may be determined experimentally.

### 3. Application to single crystal thin films under plane constrained shear

In this section, the strain gradient crystal plasticity model proposed in Section 2 is applied to study the plastic behavior of a single crystal thin film under plane constrained shear. Attention will be focused on initiation of dislocation absorption by surfaces and its effect on the strain hardening behavior. So the bulk slip resistance is neglected for brevity underlying which rigid plastic deformation is of concern although non-vanishing slip resistance can be readily solved through numerical methods.

#### 3.1. Problem description and solution

Let us consider a thin film which is infinite in the  $x_1$  direction and has finite thickness  $h$  in the direction  $x_2$  with a single active slip system defined by a slip direction  $\mathbf{s} = (\cos \theta, \sin \theta)$  and a slip plane normal  $\mathbf{m} = (-\sin \theta, \cos \theta)$ , see the Fig. 1. The film is constrained and subjected to an external shear  $\gamma^{ext}$  at the upper surface in the  $x_1$  direction, and so the boundary conditions for the displacement can be put down as

$$u_1(0) = u_2(0) = u_2(h) = 0, \quad u_1(h) = \gamma^{ext} h \quad (47)$$

The associated field displacements, plastic distortion and dislocation density depend only on  $x_2$ . From Eqs. (1)–(3), the components of the elastic strain tensor in the current context can be expressed, i.e.,

$$\begin{aligned} e_{11}^e &= \frac{1}{2} \gamma \sin 2\theta, & e_{12}^e &= e_{21}^e = \frac{1}{2} (u_{1,2} - \gamma \cos 2\theta), \\ e_{22}^e &= u_{2,2} - \frac{1}{2} \gamma \sin 2\theta \end{aligned} \quad (48)$$

where  $\gamma$  is the slip on the activated glide system. Substituting Eq. (48) into Eq. (13) yields the components of Cauchy stress tensor, i.e.,

$$\begin{aligned} \sigma_{11} &= \lambda u_{2,2} + \mu \gamma \sin 2\theta, & \sigma_{12} &= \sigma_{21} = \mu (u_{1,2} - \gamma \cos 2\theta), \\ \sigma_{22} &= (\lambda + 2\mu) u_{2,2} - \mu \gamma \sin 2\theta \end{aligned} \quad (49)$$

By taking advantage of Eq. (49), the macroscopic balance equation can be written as

$$\mu (u_{1,2} - \gamma \cos 2\theta)_{,2} = 0 \quad (50)$$

$$[(\lambda + 2\mu) u_{2,2} - \mu \gamma \sin 2\theta]_{,2} = 0 \quad (51)$$

Due to the plane constrained deformation in question, only edge GNDs are relevant and from Eq. (4), GNDs density can be expressed as

$$\rho_G^e = -\frac{1}{b} \gamma_{,2} \sin \theta \quad (52)$$

By substituting Eq. (52) into Eq. (18), the microstress reads

$$\xi = \eta R^2 \gamma_{,2} \sin \theta \mathbf{s} \quad (53)$$

with  $\eta = \mu/[8(1-\nu)]$ . Further, substituting Eqs. (19), (49) and (53) into Eq. (10) yields the microscopic balance equation, i.e.,

$$\eta R^2 \sin^2 \theta \gamma_{,22} + \mu (-\gamma + u_{1,2} \cos 2\theta + u_{2,2} \sin 2\theta) = 0 \quad (54)$$

From Eq. (45), the microtraction boundary conditions at the lower and upper surface after the surface yielding can be respectively expressed as

$$\eta R^2 \sin \theta \gamma_{,2}(0) = \Gamma_1 \text{sign}[\gamma(0)] + 2\Gamma_2 \sin^3 \theta \gamma(0) \quad (55)$$

and

$$\eta R^2 \sin \theta \gamma_{,2}(h) = -\Gamma_1 \text{sign}[\gamma(h)] - 2\Gamma_2 \sin^3 \theta \gamma(h) \quad (56)$$

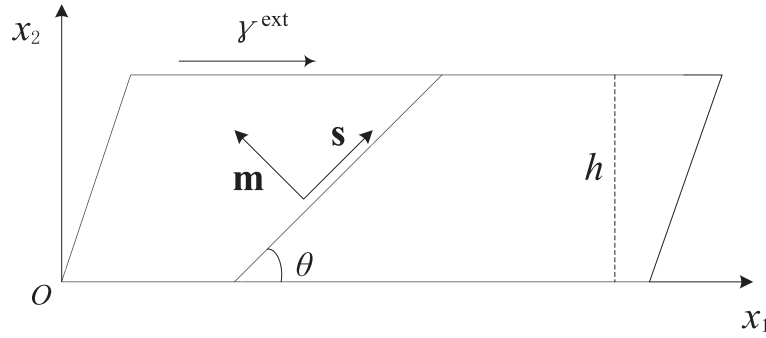


Fig. 1. Schematic for a thin film under plane constrained shear.

The solutions for displacements satisfying Eqs. (47), (50) and (51) can be obtained as

$$u_1 = (\gamma^{\text{ext}} - \langle \gamma \rangle \cos 2\theta)x_2 + \int_0^{x_2} \gamma(x) \cos 2\theta dx \quad (57)$$

$$u_2 = -\kappa \langle \gamma \rangle \sin 2\theta x_2 + \kappa \int_0^{x_2} \gamma(x) \sin 2\theta dx \quad (58)$$

where  $\kappa = \mu/(\lambda + 2\mu)$  and

$$\langle \gamma \rangle = \frac{1}{h} \int_0^h \gamma(x) dx \quad (59)$$

Substituting Eqs. (57)–(59) into Eq. (54) yields the governing equation for the slip  $\gamma$

$$\eta R^2 \sin^2 \theta \gamma_{,22} - \mu(1 - \kappa) \sin^2 2\theta \gamma - \mu(\cos^2 2\theta + \kappa \sin^2 2\theta) \langle \gamma \rangle + \mu \gamma^{\text{ext}} \cos 2\theta = 0 \quad (60)$$

to which the general solution is

$$\gamma = c_1 \exp(-\omega x_2) + c_2 \exp(\omega x_2) + c_3 \langle \gamma \rangle + c_4 \gamma^{\text{ext}} \quad (61)$$

where  $c_3 = -(\cos^2 2\theta + \kappa \sin^2 2\theta)/[(1 - \kappa) \sin^2 2\theta]$ ,  $c_4 = \cos 2\theta/[(1 - \kappa) \sin^2 2\theta]$ ,  $\omega = 4|\cos \theta|/R$ , and  $c_1, c_2$  are constants to be determined using microscopic boundary conditions.

To determine  $c_1$  and  $c_2$ , we first consider the plastic deformation before surface yielding and is termed as the stage one, so the microhard boundary condition should be adopted and in the current context becomes

$$\gamma(0) = 0, \quad \gamma(h) = 0 \quad (62)$$

Substituting Eq. (61) into Eq. (62) and Eq. (59) yields a linear system with respect to  $c_1, c_2$  and  $\langle \gamma \rangle$ , whose solutions are

$$c_1^{(1)} = \frac{1 - \exp(h\omega)}{2 \sinh(h\omega)} (c_3 \langle \gamma \rangle^{(1)} + c_4 \gamma^{\text{ext}}) \quad (63)$$

$$c_2^{(1)} = \frac{\exp(-h\omega) - 1}{2 \sinh(h\omega)} (c_3 \langle \gamma \rangle^{(1)} + c_4 \gamma^{\text{ext}}) \quad (64)$$

$$\langle \gamma \rangle^{(1)} = \frac{-\{2[1 - \cosh(h\omega)] + h\omega \sinh(h\omega)\} c_4 \gamma^{\text{ext}}}{\{2[1 - \cosh(h\omega)] + h\omega \sinh(h\omega)\} c_3 - h\omega \sinh(h\omega)} \quad (65)$$

where the superscript with brackets denotes the deformation stage. Making use of Eqs. (63)–(65) and substituting Eqs. (53) and (61) into Eq. (46), one obtains the critical value of  $\gamma^{\text{ext}}$  for surface yielding as follows

$$\gamma_{\text{cr}}^{\text{ext}} = \left| \frac{h\omega[1 + \cosh(h\omega)](1 - c_3) + 2c_3 \sinh(h\omega)}{\eta R^2 h \omega^2 c_4 \sin \theta \sinh(h\omega)} \right| \Gamma_1 \text{sign}(\gamma^{\text{ext}}) \quad (66)$$

When  $\gamma^{\text{ext}} > \gamma_{\text{cr}}^{\text{ext}}$ , the deformation of the crystalline thin film is in a stage after the surface yielding that is denoted as stage two. The microscopic surface boundary conditions Eqs. (55) and (56) should be adopted. The constants  $c_1^{(2)}, c_2^{(2)}$  and  $\langle \gamma \rangle^{(2)}$  during this stage can be expressed as

$$c_1^{(2)} = \frac{\omega h g_1 \{ \Gamma_1 \text{sign}[\gamma(0)] + 2\Gamma_2 \sin^3 \theta (c_3 \langle \gamma \rangle^{(2)} + c_4 \gamma^{\text{ext}}) \}}{1 - \exp(-h\omega)} \quad (67)$$

$$c_2^{(2)} = \frac{\omega h g_1 \{ \Gamma_1 \text{sign}[\gamma(0)] + 2\Gamma_2 \sin^3 \theta (c_3 \langle \gamma \rangle^{(2)} + c_4 \gamma^{\text{ext}}) \}}{\exp(h\omega) - 1} \quad (68)$$

$$\langle \gamma \rangle^{(2)} = -\frac{2\Gamma_1 g_1 \text{sign}[\gamma(0)] + c_4 (4\Gamma_2 \sin^3 \theta g_1 + 1) \gamma^{\text{ext}}}{c_3 (4\Gamma_2 \sin^3 \theta g_1 + 1) - 1} \quad (69)$$

where

$$g_1 = \frac{\exp(\omega h)(\eta R^2 \omega + 2\Gamma_2 \sin^2 \theta) - \exp(-\omega h)(\eta R^2 \omega - 2\Gamma_2 \sin^2 \theta) - 4\Gamma_2 \sin^2 \theta}{\omega h \sin \theta [\exp(-\omega h)(\eta R^2 \omega - 2\Gamma_2 \sin^2 \theta)^2 - \exp(\omega h)(\eta R^2 \omega + 2\Gamma_2 \sin^2 \theta)^2]} \quad (70)$$

The shear stress  $\sigma_{12}$  can be obtained by substituting Eq. (57) into Eq. (49) that is homogenous over the thickness. So during the whole deformation stage, the response of shear stress to external applied shear can be expressed as

$$\sigma_{12} = \begin{cases} \mu(\gamma^{\text{ext}} - \langle \gamma \rangle^{(1)} \cos 2\theta) & \gamma^{\text{ext}} \leq \gamma_{\text{cr}}^{\text{ext}} \\ \mu(\gamma^{\text{ext}} - \langle \gamma \rangle^{(2)} \cos 2\theta) & \gamma^{\text{ext}} > \gamma_{\text{cr}}^{\text{ext}} \end{cases} \quad (71)$$

From Eqs. (65) and (69),  $\sigma_{12}$  depends on  $\gamma^{\text{ext}}$  linearly at both stages but with different slopes.

### 3.2. Numerical results and discussion

To present numerical results based on the previous analytical solutions, let us consider the choice of the values for the associated material parameters first. The elastic constants and the magnitude of the Burgers vectors of aluminum are adopted here, i.e.,  $\mu = 26.3$  GPa,  $\nu = 0.33$  and  $b = 0.25$  nm. According to many previous works (Bittencourt et al., 2003; Fredriksson and Gudmundson, 2005; Aifantis et al., 2006; Liu et al., 2011; Aghababaei and Joshi, 2012; Mayeur and McDowell, 2013), the bulk material length scale  $R$  varies from tens of nanometers to several microns, thus we take an intermediate value here, i.e.,  $R = 0.5$   $\mu\text{m}$ . By fitting the numerical simulation results to the experiments data, Hurtado and Ortiz (2012) obtained a value of 90.0 N/m for  $\Gamma_1$  of nickel greatly in excess of the corresponding known surface free energy density, which is attributed to the considerable surface damage of the samples in experiments during the manufacturing process. In the present work, we simply choose a value of 10 N/m for  $\Gamma_1$  which

is much smaller than that in [Hurtado and Ortiz \(2012\)](#) but still larger than the usual surface free energy density for aluminum. Based on the model of surface steps as force dipoles shown in Section 2.4.2, it is reasonable to assume that the order of magnitude of  $\Gamma_2$  is same with that of  $(\Gamma_1)^2$ , and thus  $\Gamma_2 = 100 \text{ N/m}$  is adopted here. The thickness of the film  $h$  and the angle  $\theta$  between the slip direction and the  $x_1$  axis are taken as  $h = 1 \mu\text{m}$  and  $\theta = 5\pi/12$  unless otherwise stated.

Since in essence rigid plasticity of the thin film is considered in the present work, one may wonder when surface becomes penetrable to dislocations and what governs such behavior. Given the solution in Eq. (66), we have plotted  $\gamma_{cr}^{ext}$  as a function of the film thickness  $h$  in the range from 0.3 to 10  $\mu\text{m}$  in Fig. 2, where three different values for  $\theta$ , i.e.,  $\pi/6$ ,  $\pi/3$  and  $5\pi/12$  are considered. The size effect in  $\gamma_{cr}^{ext}$  is evident. With increase in film thickness  $\gamma_{cr}^{ext}$  decreases first and then increases until approaching to a steady value. This unusual size effect indicates that the surface yielding is more likely to happen within the range from 0.5 to 1  $\mu\text{m}$  in the present problem. In Fig. 3,  $\gamma_{cr}^{ext}$  as a function of  $\theta$ , i.e., the glide direction, has been presented. It can be seen that  $\gamma_{cr}^{ext}$  diverges at  $\theta = 0$  and  $\theta = \pi/4$ . When  $\theta = 0$ , the slip direction is parallel to the surface, so dislocations cannot arrive at the surface so as to form steps and consequently surface yielding will not happen. Nevertheless, the divergence at  $\theta = \pi/4$  is not necessary and is owed to the failure in satisfying the microscopic balance equation of Eq. (60). In the range of  $(0, \pi/4)$ ,  $\gamma_{cr}^{ext}$  decreases first and then increases with the increase of  $\theta$  while in the range of  $(\pi/4, \pi/2)$ ,  $\gamma_{cr}^{ext}$  decreases monotonously with the increase of  $\theta$ .

To illustrate the possible effect of surface yielding on the work hardening, the shear stress  $\sigma_{12}$  versus the external applied shear  $\gamma^{ext}$  has been calculated for the thin film thickness equal to 1, 2 and 3  $\mu\text{m}$ . Results are plotted in Fig. 4. The first stage of these curves represents the linear hardening of the crystal bulk where the surface is impenetrable due to the inadequacy of driving force for dislocations to enter the surface. After the external applied shear reaches a critical value  $\gamma_{cr}^{ext}$  marked by solid circles on the curves, the dislocations penetrate the surface resulting in surface yielding, and the crystal bulk and surface together induce linear hardening with a slope smaller than that in stage one. The smaller hardening modulus during stage two can be attributed to the dislocation absorption by the surface that weakens the dislocation pile-up, but this difference decreases rapidly as the increase of film thickness, and the “knee” of the curve almost disappears when the film thickness is large enough (see the curve when  $h = 3 \mu\text{m}$ ), which

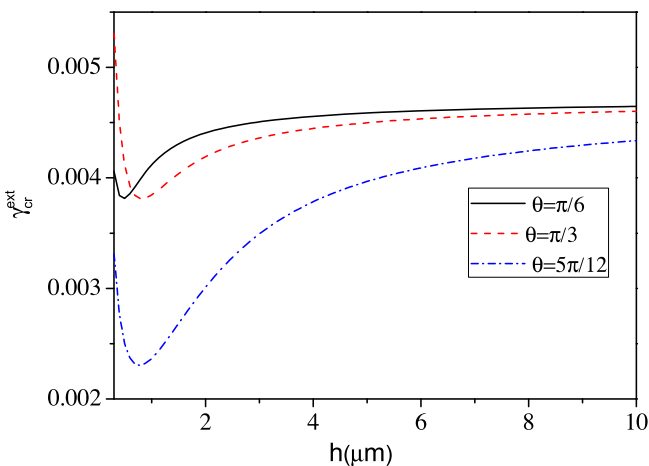


Fig. 2. Surface yield strength  $\gamma_{cr}^{ext}$  as a function of film thickness  $h$  for  $\theta = \pi/6$ ,  $\pi/3$ , and  $5\pi/12$ .

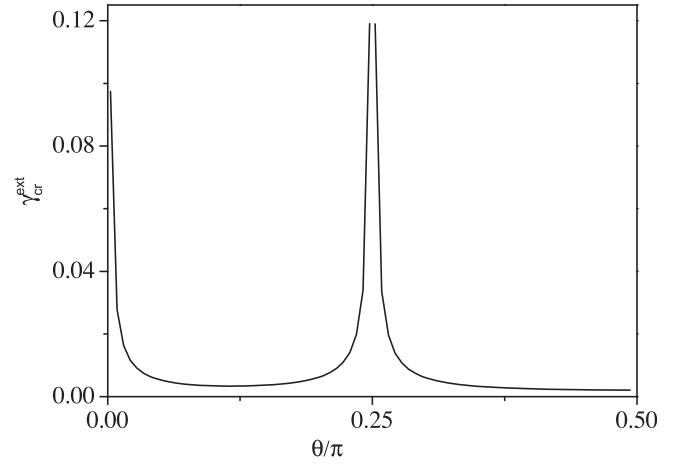


Fig. 3. Surface yield strength  $\gamma_{cr}^{ext}$  as a function of  $\theta$  for  $h = 1 \mu\text{m}$ .

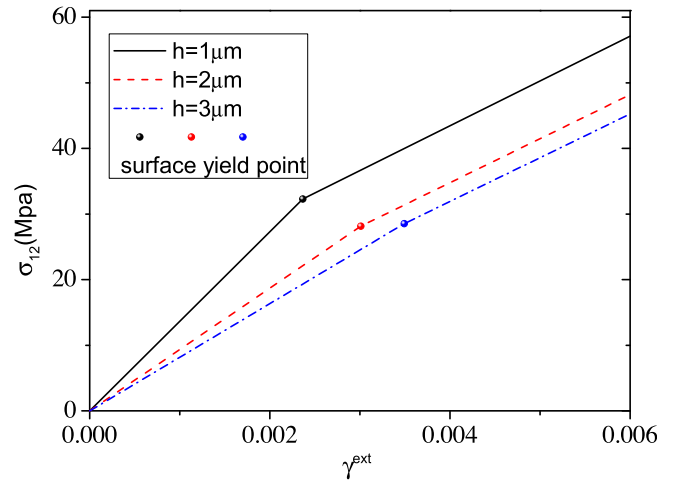


Fig. 4. Shear stress  $\sigma_{12}$  versus external applied shear  $\gamma^{ext}$  for  $h = 1, 2$  and  $3 \mu\text{m}$ .

is consistent to the fact that experimentally obtained stress–strain curve at relatively large scales usually has no obvious transition indicating the surface yielding which may indeed happen. It also indicates that the flow stress exhibits a “smaller is stronger” type size effect whose explicit expression can be found in Eq. (71).

Fig. 5 shows the distribution of slip shear for three different values of  $\gamma^{ext}$ , namely  $0.5\gamma_{cr}^{ext}$ ,  $\gamma_{cr}^{ext}$  and  $1.5\gamma_{cr}^{ext}$  which correspond to the stage before surface yielding, at the surface yielding and the stage after surface yielding respectively. It can be seen that as the increase of  $\gamma^{ext}$ , the slip  $\gamma$  at the surfaces is zero until surface yielding. The slopes of the curves can be related to the GNDs density and so one may find that the hardening is attributed to the dislocations.

It is noteworthy that the present surface energy model includes a quadratic term with respect to the plastic deformation which arises from the interaction between surface steps (see Eq. (44)) and has been overlooked in [Hurtado and Ortiz \(2012\)](#). The effect of quadratic term is expected to play a role in hardening. To elucidate the effect of this term, the distribution of slip  $\gamma$  and GNDs density  $\rho_c^e$  in the film for different values of  $\gamma^{ext}$  with  $\Gamma_2 = 100 \text{ N/m}$  has been determined and for comparison, the results from the surface model by [Hurtado and Ortiz \(2012\)](#) (i.e.,  $\Gamma_2 = 0$ ) has also been calculated, as demonstrated in Fig. 6 and Fig. 7. Note that all the values of  $\gamma^{ext}$  has been taken to ensure the occurrence of surface yielding. Since in the model by [Hurtado and Ortiz \(2012\)](#)  $\rho_c^e$  is independent of  $\gamma^{ext}$  as can be seen from Eqs. (52), (61) and (67)–

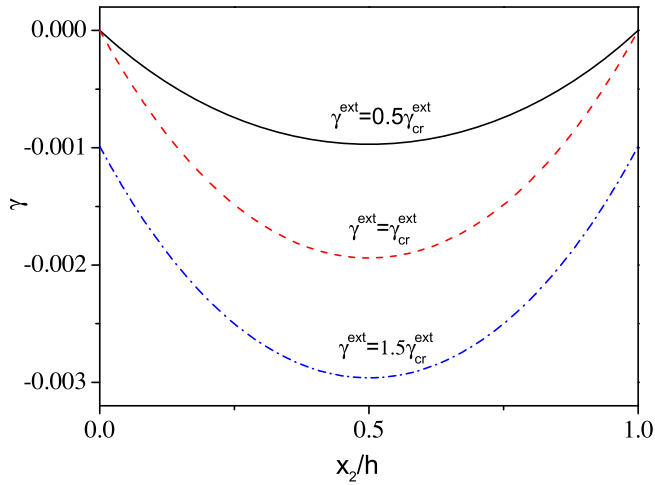


Fig. 5. Distribution of slip  $\gamma$  for  $\gamma^{\text{ext}} = 0.5\gamma_{\text{cr}}^{\text{ext}}$ ,  $\gamma_{\text{cr}}^{\text{ext}}$  and  $1.5\gamma_{\text{cr}}^{\text{ext}}$ .

(69), only one curve for the distribution of  $\rho_G^e$  in this situation is plotted. From Fig. 6, the effect of the quadratic term on the distribution of  $\gamma$  is not obvious even when  $\gamma^{\text{ext}}$  is as large as 10%. However, its effect on the distribution of  $\rho_G^e$  can be significant when  $\gamma^{\text{ext}}$  is relatively large. Therefore, the effect of surface step induced elastic energy may be negligible for quite small deformation and should be taken into account for relatively larger deformation.

Conventionally, within strain gradient plasticity, the microhard and microfree models have been adopted in the literature. Herein we have proposed a new surface model which gives boundary conditions naturally. To compare the present surface model with the conventional models, the plastic response of the thin film under corresponding three different surface boundary conditions has been considered. The solution for the case of microhard condition is given in Eq.(61) and Eqs. (63)–(65), and the solution for the case of microfree condition can be obtained from the present solution by taking  $\Gamma_1 = \Gamma_2 = 0$ . The distribution of  $\gamma$  and  $\rho_G^e$  over the thickness of the film at  $\gamma^{\text{ext}} = 5\gamma_{\text{cr}}^{\text{ext}}$  are plotted in Figs. 8 and 9 respectively. It can be seen that the difference among these three different surface models are remarkable. Distribution of  $\gamma$  for the case of microhard condition is most highly inhomogeneous and  $\rho_G^e$  is larger at the surface with strong dislocation pile-up. As the

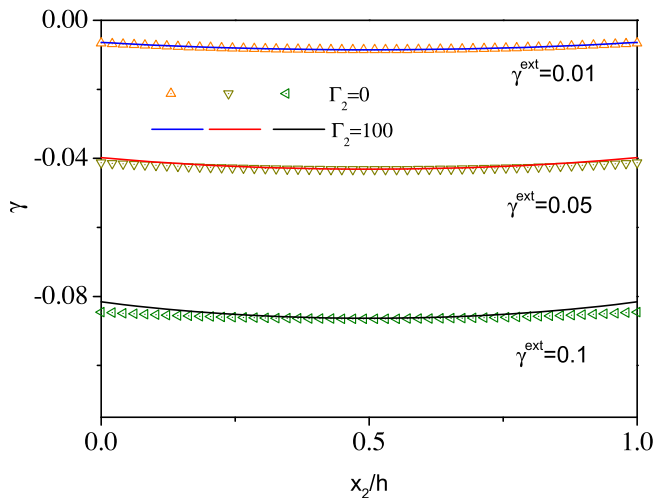


Fig. 6. Comparison of distribution of slip  $\gamma$  by present surface model ( $\Gamma_2 = 100 \text{ N/m}$ ) with that by Hurtado and Ortiz (2012) model ( $\Gamma_2 = 0$ ) for  $\gamma^{\text{ext}} = 0.01, 0.05$  and  $0.1$ .

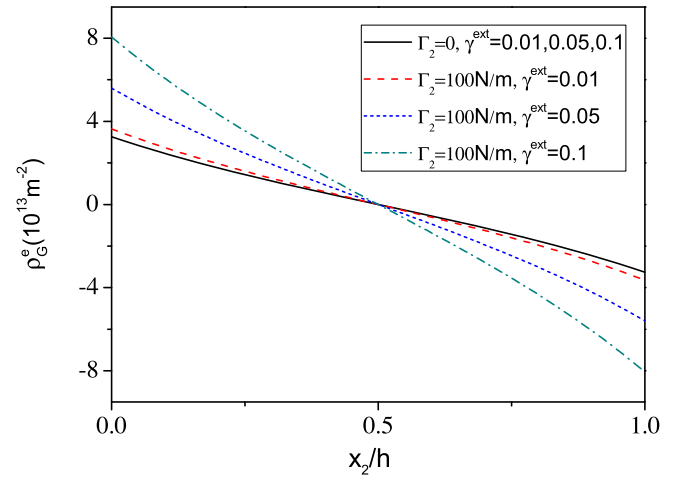


Fig. 7. Comparison of distribution of GNDs density  $\rho_G^e$  by present surface model ( $\Gamma_2 = 100 \text{ N/m}$ ) with that by Hurtado and Ortiz (2012) model ( $\Gamma_2 = 0$ ) for  $\gamma^{\text{ext}} = 0.01, 0.05$  and  $0.1$ .

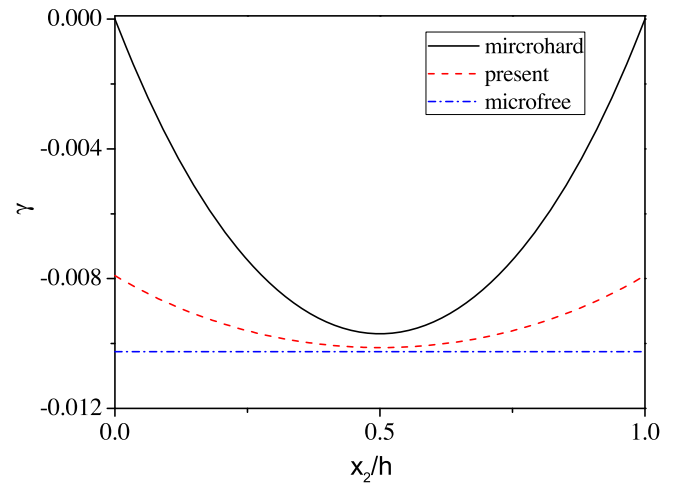


Fig. 8. Distribution of slip  $\gamma$  by present surface model, microhard and microfree models for  $\gamma^{\text{ext}} = 5\gamma_{\text{cr}}^{\text{ext}}$ .

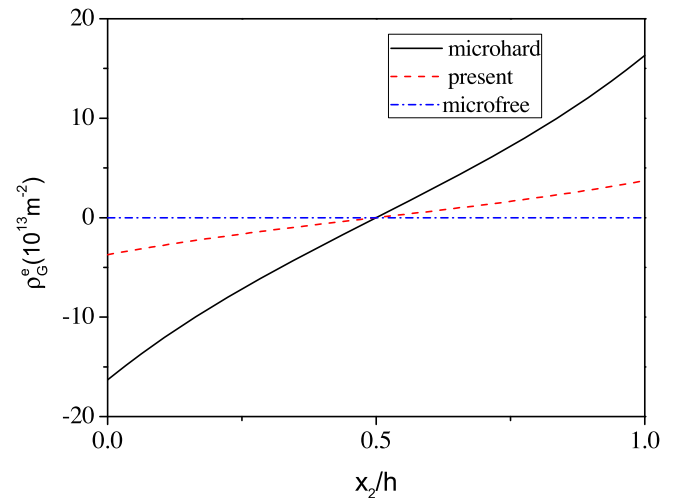
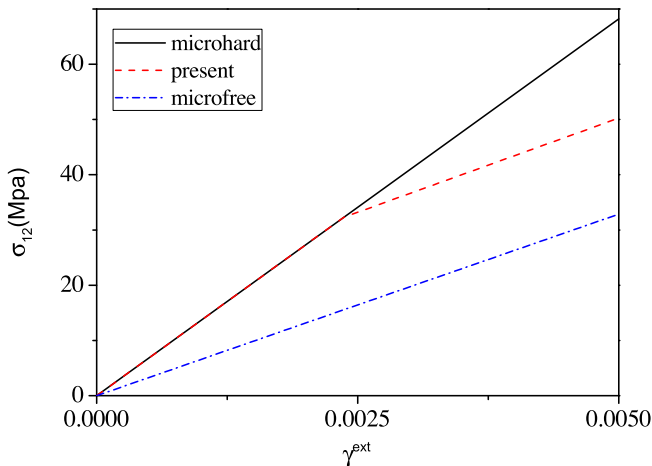


Fig. 9. Distribution of GNDs density  $\rho_G^e$  by present surface model, microhard and microfree models for  $\gamma^{\text{ext}} = 5\gamma_{\text{cr}}^{\text{ext}}$ .





**Fig. 10.** Shear stress  $\sigma_{12}$  versus external applied shear  $\gamma^{\text{ext}}$  curves by present surface model, microhard and microfree models.

surface is free for dislocation to escape for the case of microfree condition, there is no dislocation within the film at the steady state and distribution of slip shear is homogeneous. For the present model, dislocations are permitted to penetrate the surface gradually but not freely after the surface yielding, thus  $\rho_s^c$  at the surface is not zero but smaller than that of the microhard case. The shear stress versus the external applied shear curves for the three surface models are plotted in Fig. 10 which indicates distinct hardening behaviors. Thus, to better capture the plastic behaviors of crystals by means of crystal plasticity theory model, choosing proper boundary conditions is very important. And the present model may provide such an opportunity when the surface is penetrable to dislocations.

#### 4. Conclusions

In this paper, a physically motivated strain gradient model for single crystal plasticity has been developed. Based on the physical fact that the surface steps form after dislocation penetration, an energetic surface model has been proposed by considering the energy from the increase in surface area and that due to interaction between surface steps. A yield condition for surface can be obtained naturally. As an application, plastic behavior of a thin film under plane constrained shear have been studied with the present model. It is found that yield strength of the surface strongly depends on the film thickness and the relative orientation between the slip system and the surface. Comparing the results calculated by the present surface model with those by the microhard and microfree models, the plastic behavior is found to be sensitive to the microscopic boundary conditions, indicating that a proper surface model is very important for a crystal plasticity theory in order to well describe the plastic behavior of crystals. It can be concluded that the present model may be efficient in capturing the dislocation absorption by surfaces and hence predicting the onset of mechanical annealing but may fail to consider the onset of plastic deformation mediated by surfaces given the presently adopted bulk constitutive assumptions. Moreover, it is likely that dislocation absorption by surfaces may involve dissipative processes which may beyond capture of the present model in the current form. Those altogether require further improvement of the present model which should be based on additional details on the relevant deformation processes.

#### Acknowledgment

The support by the National Key Basic Research Scheme of China under Grant No. 2012CB937500 is gratefully acknowledged.

#### References

- Abu Al-Rub, R.K., 2008. Modeling the interfacial effect on the yield strength and flow stress of thin metal films on substrates. *Mech. Res. Commun.* 35, 65–72.
- Acharya, A., Bassani, J.L., 2000. Lattice incompatibility and a gradient theory of crystal plasticity. *J. Mech. Phys. Solids* 48, 1565–1595.
- Aghababaei, R., Joshi, S.P., 2012. A crystal plasticity analysis of length-scale dependent internal stresses with image effects. *J. Mech. Phys. Solids* 60, 2019–2043.
- Aifantis, E.C., 1984. On the microstructural origin of certain inelastic models. *J. Eng. Mater. Tech.* 106, 326–330.
- Aifantis, K.E., Soer, W.A., De Hosson, J.T.M., Willis, J.R., 2006. Interfaces within strain gradient plasticity: theory and experiments. *Acta Mater.* 54, 5077–5085.
- Bayley, C.J., Brekelmans, W.A.M., Geers, M.G.D., 2006. A comparison of dislocation induced back stress formulations in strain gradient crystal plasticity. *Int. J. Solids Struct.* 43, 7268–7286.
- Bittencourt, E., Needleman, A., Gurtin, M.E., Van der Giessen, E., 2003. A comparison of nonlocal continuum and discrete dislocation plasticity predictions. *J. Mech. Phys. Solids* 51, 281–310.
- Cermelli, P., Gurtin, M.E., 2002. Geometrically necessary dislocations in viscoplastic single crystal and bicrystals undergoing small deformation. *Int. J. Solids Struct.* 39, 6281–6309.
- Chen, S.H., Wang, T.C., 2000. A new hardening law for strain gradient plasticity. *Acta Mater.* 48, 3997–4005.
- Ertürk, I., van Dommelen, J.A.W., Geers, M.G.D., 2009. Energetic dislocation interactions and thermodynamical aspects of strain gradient crystal plasticity theories. *J. Mech. Phys. Solids* 57, 1801–1814.
- Evers, L.P., Parks, D.M., Brekelmans, W.A.M., Geers, M.G.D., 2002. Crystal plasticity model with enhanced hardening by geometrically necessary dislocation accumulation. *J. Mech. Phys. Solids* 50, 2403–2424.
- Evers, L.P., Brekelmans, W.A.M., Geers, M.G.D., 2004. Non-local crystal plasticity model with intrinsic SSD and GND effects. *J. Mech. Phys. Solids* 52, 2379–2401.
- Fleck, N.A., Hutchinson, J.W., 1993. A phenomenological theory for strain gradient effects in plasticity. *J. Mech. Phys. Solids* 41, 1825–1857.
- Fleck, N.A., Muller, G.M., Ashby, M.F., Hutchinson, J.W., 1994. Strain gradient plasticity: theory and experiment. *Acta Metall. Mater.* 42, 475–487.
- Fleck, N.A., Hutchinson, J.W., 1997. Strain gradient plasticity. *Adv. Appl. Mech.* 33, 295–361.
- Fredriksson, P., Gudmundson, P., 2005. Size-dependent yield strength of thin films. *Int. J. Plast.* 21, 1834–1854.
- Fredriksson, P., Gudmundson, P., 2007. Competition between interface and bulk dominated plastic deformation in strain gradient plasticity. *Model. Simul. Mater. Sci. Eng.* 15, S61–S69.
- Groma, I., Csikor, F.F., Zaiser, M., 2003. Spatial correlations and higher-order gradient terms in a continuum description of dislocation dynamics. *Acta Mater.* 51, 1271–1281.
- Gu, X.W., Loynachan, C.N., Wu, Z., Zhang, Y.W., Srolovitz, D.J., Greer, J.R., 2012. Size-dependent deformation of nanocrystalline Pt nanopillars. *Nano Lett.* 12, 6385–6392.
- Gudmundson, P., 2004. A unified treatment of strain gradient plasticity. *J. Mech. Phys. Solids* 52, 1379–1406.
- Gurtin, M.E., 2000. On the plasticity of single crystals: free energy, microforces, plastic-strain gradients. *J. Mech. Phys. Solids* 48, 989–1036.
- Gurtin, M.E., 2002. A gradient theory of single-crystal viscoplasticity that accounts for geometrically necessary dislocations. *J. Mech. Phys. Solids* 50, 5–32.
- Gurtin, M.E., Needleman, A., 2005. Boundary conditions in small-deformation, single-crystal plasticity that account for the Burgers vector. *J. Mech. Phys. Solids* 53, 1–31.
- Han, C.-S., Gao, H., Huang, Y., Nix, W.D., 2005. Mechanism-based strain gradient crystal plasticity—I. Theory. *J. Mech. Phys. Solids* 53, 1188–1203.
- Huang, G.-Y., Svendsen, B., 2010. Effect of surface energy on the plastic behavior of crystalline thin films under plane strain constrained shear. *Int. J. Fracture* 166, 173–178.
- Hurtado, D.E., Ortiz, M., 2012. Surface effects and the size-dependent hardening and strengthening of nickel micropillars. *J. Mech. Phys. Solids* 60, 1432–1446.
- Kacher, J., Eftink, B.P., Cui, B., Robertson, I.M., 2014. Dislocation interactions with grain boundaries. *Curr. Opin. Solid State Mater. Sci.* 18, 227–243.
- Kuroda, M., Tvergaard, V., 2008. On the formulations of higher-order strain gradient crystal plasticity models. *J. Mech. Phys. Solids* 56, 1591–1608.
- Liu, Z.-L., Zhuang, Z., Liu, X.-M., Zhao, X.-C., Gao, Y., 2011. Bauschinger and size effects in thin-film plasticity due to defect-energy of geometrical necessary dislocations. *Acta Mech. Sin.* 27, 266–276.
- Marchenko, V.I., Parshin, A.Y., 1980. Elastic properties of crystal surfaces. *Sov. Phys. JETP* 52, 129–131.
- Mayeur, J.R., McDowell, D.L., 2013. An evaluation of higher-order single crystal strength models for constrained thin films subjected to simple shear. *J. Mech. Phys. Solids* 61, 1935–1954.

- McElhane, K.W., Vlassak, J.J., Nix, W.D., 1998. Determination of indenter tip geometry and indentation contact area for depth-sensing indentation experiments. *J. Mater. Res.* 13, 1300–1306.
- Müller, P., Saúl, A., 2004. Elastic effects on surface physics. *Sur. Sci. Rep.* 54, 157–258.
- Oh, S.H., Legros, M., Kiener, D., Dehm, G., 2009. In situ observation of dislocation nucleation and escape in a submicrometre aluminium single crystal. *Nat. Mater.* 8, 95–100.
- Prévot, G., Croset, B., 2004. Revisiting elastic interactions between steps on vicinal surfaces: the buried dipole model. *Phys. Rev. Lett.* 92, 256104.
- Prévot, G., Croset, B., 2006. Elastic relaxations and interactions on metallic vicinal surfaces: testing the dipole model. *Phys. Rev. B* 74, 235410.
- Rabkin, E., Srolovitz, D.J., 2007. Onset of plasticity in gold nanopillar compression. *Nano Lett.* 7, 101–107.
- Rajabzadeh, A., Mompou, F., Legros, M., Combe, N., 2013. Elementary mechanisms of shear-coupled grain boundary migration. *Phys. Rev. Lett.* 110, 265507.
- Shan, Z.W., Mishra, R.K., Syed Asif, S.A., Warren, O.L., Minor, A.M., 2008. Mechanical annealing and source-limited deformation in submicrometre-diameter Ni crystals. *Nat. Mater.* 7, 115–119.
- Sieradzki, K., Rinaldi, A., Friesen, C., Peralta, P., 2006. Length scales in crystal plasticity. *Acta Mater.* 54, 4533–4538.
- Spearot, D.E., Jacob, K.L., McDowell, D.L., 2005. Nucleation of dislocations from [001] bicrystal interfaces in aluminum. *Acta Mater.* 53, 3579–3589.
- Spearot, D.E., Sangid, M.D., 2014. Insights on slip transmission at grain boundaries from atomistic simulations. *Curr. Opin. Solid State Mater. Sci.* 18, 188–195.
- Swadener, J.G., George, E.P., Pharr, G.M., 2002. The correlation of the indentation size effect measured with indenters of various shapes. *J. Mech. Phys. Solids* 50, 681–694.
- Van Swygenhoven, H., Derlet, P., Hasnaoui, A., 2002. Atomic mechanism for dislocation emission from nanosized grain boundaries. *Phys. Rev. B* 66, 024101.
- Wang, J., Misra, A., Hoagland, R.G., Hirth, J.P., 2012a. Slip transmission across fcc/bcc interfaces with varying interface shear strengths. *Acta Mater.* 60, 1503–1513.
- Wang, Z.-J., Li, Q.-J., Shan, Z.-W., Li, J., Sun, J., Ma, E., 2012b. Sample size effects on the large strain bursts in submicron aluminum pillars. *Appl. Phys. Lett.* 100, 071906.
- Yefimov, S., Groma, I., van der Giessen, E., 2004. A comparison of a statistical-mechanics based plasticity model with discrete dislocation plasticity calculations. *J. Mech. Phys. Solids* 52, 279–300.

- Yuasa, M., Nakazawa, T., Mabuchi, M., 2010. Atomic simulations of dislocation emission from Cu/Cu and Co/Cu grain boundaries. *Mater. Sci. Eng. A* 528, 260–267.



Dr. Gan-Yun Huang, Professor at Department of Mechanics, School of Mechanical Engineering, Tianjin University, Tianjin, P.R. China. His research interests cover mechanical modeling of small-scaled materials via non-local models, contact mechanics, friction and material failure models.



Xiang-Long Peng, Ph.D student of solid mechanics at Department of Mechanics, School of Mechanical Engineering, Tianjin University, Tianjin, P.R. China. His research interests focus on modelling of mechanical behavior of materials and structures at micron/-nanometer scales.